OFDM/FM Frame Synchronization for Mobile Radio Data Communication

William D. Warner and Cyril Leung, *Member, IEEE*

Abstract— **A synchronization scheme enabling the use of orthogonal frequency division multiplexing OFDM/FM over a mobile radio channel in a pure ALOHA environment is proposed. The scheme encodes synchronization information in parallel with data in the same manner in which data is encoded in the OFDM/FM frame. The synchronization information is in the form of tones, centered in certain reserved frequency sub-channels of the OFDM signal. The receiver uses a correlation detector, implemented in the frequency domain, to acquire synchronization accurately on a packet-by-packet basis. Experimental results indicate that the bit-error-rate performance achievable with the proposed scheme is within 1.5 dB of the performance obtained with ideal synchronization.**

I. Introduction

DIGITAL communication over VHF/UHF mobile radio channels is a topic of great current interest. Applications include cellular telephone systems [1]; mobile data terminals (MDT's), which are used to streamline business operations; public-safety and rescue services; and 'tetherless' personal communication systems of the future [2], [3]. The benefits provided by digital communication include: (1) improved utilization of the radio spectrum; (2) increased reliability in communicating information that is very sensitive to channel errors; (3) direct access to computerized databases, resulting in greater operational efficiency and reduced delays; (4) a high degree of confidentiality and integrity provided by the use of encryption techniques; and (5) integration of voice and data services.

In most urban and many suburban areas, one of the main obstacles to efficient and reliable data communication over a VHF/UHF mobile radio channel is multipath propagation, which results in severe and rapid fluctuations in the received signal strength. Theoretical and experimental studies [4], [5] have shown that the amplitude of the received fading signal is well approximated by a Rayleigh distribution over short distances, typically a few tens of meters. Over larger distances, shadowing of the received signal by hills and other large obstacles results in a log-normal variation in the mean of the Rayleigh distribution [5], [6]. Generally, the Rayleigh fades impose the most severe constraints on digital communication.

Manuscript received July 15, 1992; revised December 1, 1992. This work was supported in part by an NSERC post-graduate scholarship, a B.C. Science Council GREAT award, and by NSERC under Grant OGP0001731.

W. D. Warner is with MPR Teltech Ltd., Burnaby, BC, Canada V5A 4B5.
C. Leung is with the Department of Electrical Engineering, University of British Columbia, Vancouver, BC, Canada V6T 1Z4.

IEEE Log Number 9208474.

In a conventional serial modulation scheme in which bits (symbols) are transmitted over the channel one after another, a deep fade will result in the destruction of the affected bits. Cimini [7] has proposed the use of an orthogonal frequency division multiplexing (OFDM) scheme in which a block of bits is transmitted in parallel, each at a low baud rate. The basic idea behind the scheme is to spread out the effect of a fade over many bits. Rather than have a few adjacent bits completely destroyed by a fade, we now have all the bits slightly affected. More recently, an OFDM/FM scheme has been studied [8]. OFDM/FM is particularly attractive because it can be implemented simply and inexpensively by retrofitting existing FM communication systems.

In [7] and [8], the problem of symbol (frame) synchronization was not addressed. In this paper, a technique for achieving this synchronization for an OFDM/FM system is proposed and experimentally evaluated.

II. Preliminaries

In this section, OFDM modulation is first briefly reviewed. Characteristics of the FM mobile radio fading channel pertinent to the synchronization problem are then discussed.

A. OFDM Principles of Operation

In OFDM, the sub-carrier frequencies are chosen to be spaced at the symbol rate; that is, if the OFDM symbol duration is T seconds, the sub-carrier frequency spacing is $1/T$ Hz. With this frequency spacing, the sub-carriers are orthogonal over one symbol interval [9], [10].

Data to be transmitted are grouped into blocks of K bits. A smaller grouping of bits (usually two to five) is assigned to each sub-carrier. Typically, a 2^m-QAM (Quadrature Amplitude Modulation) constellation is used to encode the data into the phase and magnitude of the sub-carrier, where m is the number of bits assigned to the sub-carrier.[1]

Modulation and demodulation can be done efficiently using a fast Fourier transform (FFT) algorithm [10]. More specifically, the modulating signal is obtained as follows: The m-bit groupings of data are encoded as complex values, $a + jb$, defining points in the 2^m -QAM constellation. These complex values are input to an N-point inverse FFT (IFFT) algorithm, with their location in the IFFT data array corresponding to their assigned sub-carrier channel position in frequency. If specific sub-carriers are not used, the corresponding values

[1] In general, the number of bits assigned to each sub-carrier can vary from one sub-carrier to the next [11].

0018–9598/93$03.00 © 1993 IEEE

Authorized licensed use limited to: Oxford University Libraries. Downloaded on March 31,2010 at 11:34:57 EDT from IEEE Xplore. Restrictions apply.

in the IFFT data array are set to zero. Only the lower half of the data array can be independently specified. The upper half of the data array is set equal to the complex conjugate of the lower half, so as to produce a set of N *real* modulating signal samples when the IFFT is performed. These *real* signal samples are then converted to an analog modulating waveform using appropriate *digital-to-analog* (D/A) converters and reconstruction filters. In OFDM/FM, this waveform is used to modulate an FM transmitter.

At the receiver, the recovered baseband signal is sampled and converted to digital form. N consecutive samples are grouped to form an OFDM block. An N-point FFT is performed to determine the phase and magnitude of each sub-carrier. For each sub-carrier, the transmitted information is extracted by determining the signal point closest to the point corresponding to the received sub-carrier. This signal point then identifies the transmitted m-bit data sequence.

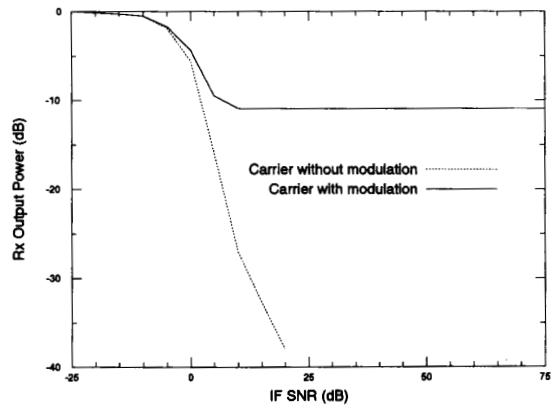

Fig. 1. Receiver output power versus IF S/N.

B. FM Fading Channel

Proper design of a synchronization scheme for OFDM/FM requires knowledge of the characteristics of the FM radio transmitter–receiver (transceiver) used. Two ICOM-2AT transceivers [12] are used for the experimental work, one as the transmitter and one as the receiver. An operating frequency of 144.15 MHz was chosen. FM transceiver characteristics were as follows:

1) Transient Response: An abrupt change in the modulating signal, such as encountered at the start of the signal, gives rise to transients in the transmitted RF signal. Likewise, when the receiver experiences abrupt changes in the modulation of the received carrier signal, transients are generated. These transients result in a distorted received signal, which degrades the orthogonality of the sub-carriers in the OFDM baseband signal. Therefore, it is important to allow the transients to decay before demodulation is performed. This was ensured by preceding the OFDM modulating signal with a periodic extension of the signal itself. Measurements of the transient response of the ICOM-2AT transceiver pair indicated that a pre-extension duration of 4 ms would be adequate. This corresponds to 32 samples at the 8-kHz sampling rate used in the experiments. For an OFDM block size of 1024 samples, this represents an overhead of approximately 3%.

2) FM Channel Attack Time: Radio attack time is usually specified separately for the transmitter and receiver [13], [14], [15]. It can be a major source of transmission overhead, as modulation cannot start until the transmitter RF carrier has attained a certain power level and the receiver output power has stabilized. A longer radio attack time requires a larger "wait" time. This can severely limit efficiency, especially in systems with small packet lengths.

We are interested in the combined attack time for the Transmitter-Receiver system and will refer to it as the FM Channel Attack Time. The FM Channel Attack Time is defined as the time required for the receiver audio output power to reach its steady-state value after operation of the transmitter control switch. For the ICOM-2AT transmitter-receiver system, the FM Channel Attack Time was measured to be approximately 80 ms.

3) Receiver Output Power: When the receiver squelch is disabled, the audio output power of the ICOM-2AT receiver is greater in the absence than in the presence of a (modulated or unmodulated) carrier. Fig. 1 shows the receiver audio output power in the presence of OFDM modulated and unmodulated carriers at various IF S/N levels.

4) Baseband Noise Power Spectrum: The expression for the noise power spectrum $W(f)$ at the output of an FM discriminator is quite complicated [5]. For our discussion, it suffices to note that for f less than about half the IF bandwidth, $W(f)$ can be characterized as follows: At high IF S/N's, $W(f)$ increases as f^2, whereas at low IF S/N's, $W(f)$ varies little with f. Because the ICOM-2AT transceiver (as most FM transceivers) is designed to operate in a high IF S/N environment, the transmitter incorporates a +20-dB-per-decade standard pre-emphasis filter; a corresponding -20-dB-per-decade de-emphasis filter is present in the receiver.

In a fading environment, the IF S/N fluctuates, and there are times when it will be low. As a result, the baseband noise spectrum at the output of the ICOM-2AT receiver (after de-emphasis) may no longer be flat. To illustrate this effect, an OFDM modulating signal, in which power is distributed evenly across its spectrum, was transmitted over the fading FM channel at an IF S/N of 10 dB and a Doppler rate[2] of 10 Hz. Fig. 2 shows that the signal mean is constant over the band, whereas the noise power tends to be smaller for the higher frequency sub-channels. Casas [8] determined that using a -10 -dB-per-decade pre-emphasis (in addition to the built-in +20-dB-per-decade standard pre-emphasis) tended to equalize the S/N's of the received signal sub-channels. This additional pre-emphasis was also used in our experiments. The result of applying this additional pre-emphasis to the modulating signal is shown in Fig. 3 and results in a more constant S/N over the band.

[2]The Doppler rate, f_d, is given by $f_d = f_c v/c$, where f_c is the carrier frequency, v is the vehicle speed, and c is the velocity of light.

Authorized licensed use limited to: Oxford University Libraries. Downloaded on March 31,2010 at 11:34:57 EDT from IEEE Xplore. Restrictions apply.

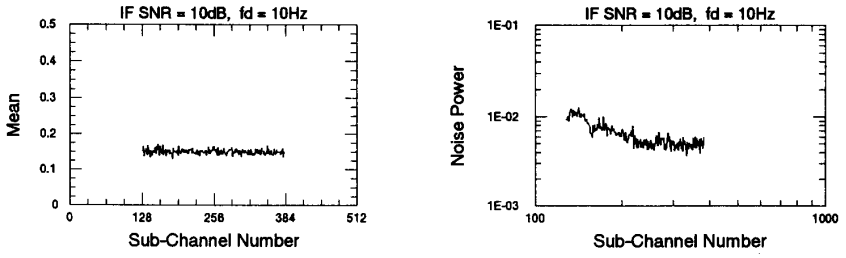

Fig. 2. Noise power distribution for modulating signal with constant power across spectrum.

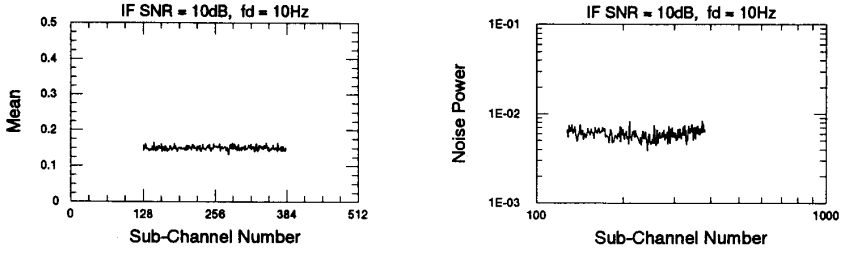

Fig. 3. Noise power distribution for modulating signal with −10-dB-per-decade pre-emphasis.

To maximize the attainable bit rate at a given error rate and S/N, Bingham [11] has indicated that the optimum power distribution should be calculated by a "water-pouring" procedure that is similar to that of Gallager [16]. Alternatively, bit error rates (BER's) can be equalized over the sub-channels by employing a technique known as adaptive loading [11]. In this technique, more bits are assigned to the sub-channels with higher S/N, and fewer bits are assigned to the sub-channels with lower S/N.

5) Channel Hardware Equalization: In Fig. 4, a block diagram of the OFDM/FM data communication system is shown. This digital FM channel accepts a stream of serial digital data. The data are processed to generate a digital signal defining the OFDM baseband modulating signal. The digital OFDM signal is passed through a D/A converter and appropriate analog reconstruction filters and gain units to yield an analog OFDM signal suitable for modulating the FM transmitter. At the receiving end, the inverse functions are performed.

The hardware comprising the digital FM channel, specifically the analog components, introduce phase and amplitude distortions which must be accounted for when decoding the OFDM signal. To measure the compensation required, a training procedure is performed in which known blocks of pseudo-random data are transmitted to the receiver. The received data blocks are then compared to the transmitted data blocks to determine the corrections required to counteract the phase and magnitude distortions. The corrections are actually implemented in software at the receiver.

The effect of channel equalization can be seen from a comparison of Fig. 5 (no equalization) and 6 (with equalization). Both figures are scatter plots of 4-QAM encoded data extracted from a received OFDM signal with IF S/N = 15 dB and no fading. It can be seen that with channel equalization, the received data points are clustered around the four QAM constellation points. Without channel equalization, the data points are scattered, and the constellation points are not evident.

III. OFDM/FM Synchronization

The synchronization requirements are first defined. The proposed synchronization technique is then discussed. Its computational requirements are modest, allowing for an economical implementation.

A. Synchronization Requirements

The synchronization technique is to be used in a pure ALOHA fading mobile FM radio environment with the following requirements: (1) Due to the pure ALOHA environment, each OFDM frame has to be synchronized independently. (2) Since the available spectrum is limited, the bandwidth overhead should be small.

Synchronization schemes devised for parallel (OFDM) transmission over telephone channels have been previously studied [17], [18], [19]. However, these schemes rely on several consecutive frames to maintain correct timing and do not meet the first requirement. Moose [20] has studied a technique for use in mobile satellite communications. In this technique, a synchronization frame is used to provide synchronization for a group of ensuing data frames. Thus synchronization is not achieved by individual data frames.

The events of interest in assessing the performance of a synchronization technique are: (1) *false alarm,* which occurs if the synchronization algorithm indicates the presence of a data block when none is present; (2) *miss detection,* which occurs if the synchronization algorithm does not detect the presence of a

Authorized licensed use limited to: Oxford University Libraries. Downloaded on March 31,2010 at 11:34:57 EDT from IEEE Xplore. Restrictions apply.

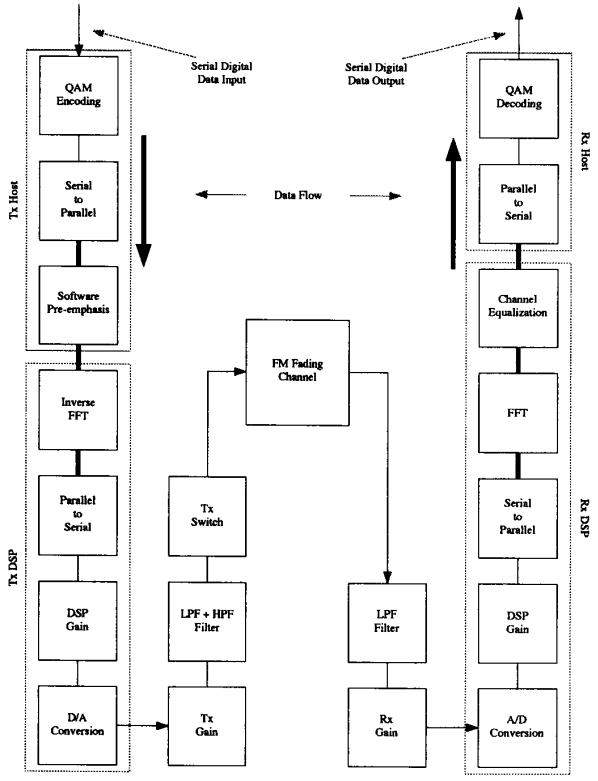

Fig. 4. Digital FM channel.

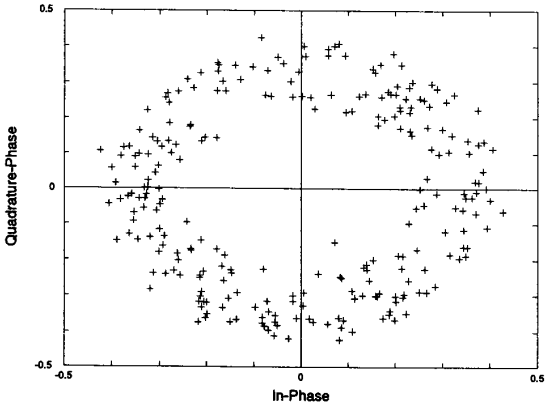

Fig. 5. Scatter plot of received data without channel equalization.

data block when one is present; (3) *bad synchronization,* which occurs if the synchronization algorithm detects the presence of a data block when one is present, but does not correctly synchronize. This occurs when distortion of the signal is enough to prevent proper synchronization, but not so bad as to cause a miss detection; and (4) *correct synchronization,* which occurs if the sychronization algorithm detects the presence of a data block when one is present and correctly synchronizes to the data block.

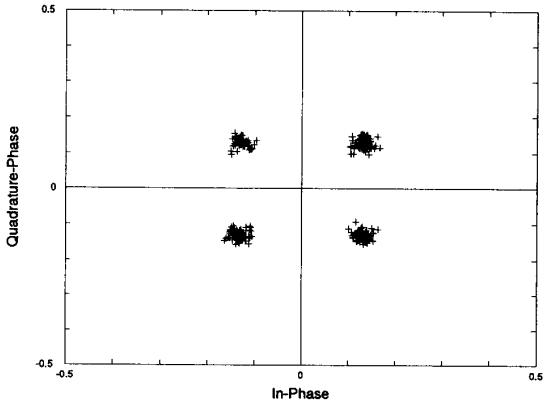

Fig. 6. Scatter plot of received data with channel equalization.

Prior to the experiments, synchronization performance objectives were established. The primary motivation is to define a level of synchronization performance such that the resulting inaccuracy in the synchronization procedure is not the major factor limiting the achievable BER. That is, the achievable BER should be limited by the OFDM modulation technique, rather than by the synchronization procedure. The target probability of false alarm, miss detection, or bad synchronization is set equal to the BER of the OFDM/FM system given ideal synchronization. This ensures that the BER with the synchronization procedure does not exceed twice the BER given ideal synchronization.

B. Proposed Synchronization Technique

In the proposed synchronization technique for OFDM/FM, the transmitter encodes a number of reserved sub-channels with known phases and amplitudes. The remaining sub-channels are encoded with data as outlined in section II-A. The technique does not rely on an accurate time–domain detection of the start of the data block and is, therefore, relatively insensitive to channel fading. Its performance depends on the number of synchronization sub-channels. For a given number of synchronization sub-channels, performance can be improved through judicious selection of sub-channels.

The technique uses three stages to achieve synchronization (see Fig. 7). Phase I detects when an OFDM signal is present by monitoring the power in the received signal. It does not attempt to acquire synchronization, but merely obtains a rough estimate of the location of the signal. In Phase II, a correlation detector is used to extract the synchronization information from the received signal and to acquire synchronization to within $\pm\frac{1}{2}$ of the sample period. Phase III provides fine-tuning by accurately locating the local peak of the correlation detector implemented in Phase II.

1) Phase I—Power Detection: It can be seen from Fig. 1 that the audio output power of the receiver is larger in the absence than in the presence of a (modulated or unmodulated) carrier. In an ALOHA mobile radio environment, a transmitter only generates a carrier when transmitting data. The receiver

Authorized licensed use limited to: Oxford University Libraries. Downloaded on March 31,2010 at 11:34:57 EDT from IEEE Xplore. Restrictions apply.

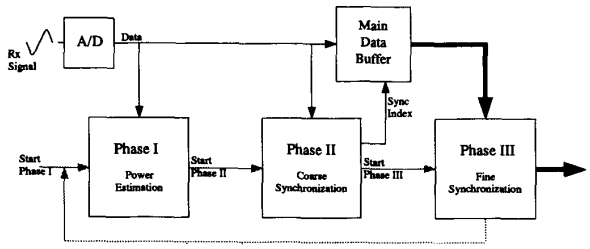

Fig. 7. Synchronization block diagram.

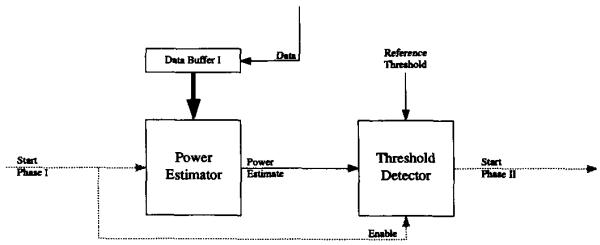

Fig. 8. Synchronization—Phase I.

audio output power can therefore be used as an indicator of the presence or absence of a data frame.

Referring to Fig. 7, the audio output power level is constantly monitored during phase I. When the power level drops below a certain threshold, it is assumed that an OFDM signal is present, and Phase II is initiated.

Fig. 8 shows in greater detail the operation of Phase I. The received data samples are stored in Data Buffer I prior to power estimation. The data buffer keeps a record of the most recent values. When a new data value is received from the A/D converter, it is loaded into Data Buffer I, and the oldest data value in the buffer is discarded. A new estimate of the output power level is obtained using

$$p = \sum_{i=0}^{N_s-1} (x_i)^2 \tag{1}$$

where x_i are the data samples and N_s is the number of samples used in the estimate. The choice of N_s involves a trade-off between reliability and responsiveness to changes in the output power. As a compromise, N_s is set equal to N, the number of samples in the OFDM frame.

If the threshold is set too high, the result will be a high probability of false alarm. On the other hand, a threshold which is set too low will result in a high probability of miss detection. An appropriate threshold value was determined experimentally as discussed in Section V-A.

2) Phase II—Coarse Synchronization Phase II is used to acquire synchronization alignment to within $\pm\frac{1}{2}$ sample period. This is considered to be coarse synchronization because it is unacceptable for the decoding of the OFDM data. Consider the data sub-carrier corresponding to 2 kHz, the center of the OFDM baseband signal (see *OFDM Signal Generation* in Section IV-A(1)). At a sampling rate of 8 kHz, an alignment error of $\pm\frac{1}{2}$ of a sampling period will result in a phase error of ± 45 degrees, which is unacceptable for QAM decoding. For higher frequency data sub-carriers, the phase errors will be even greater.

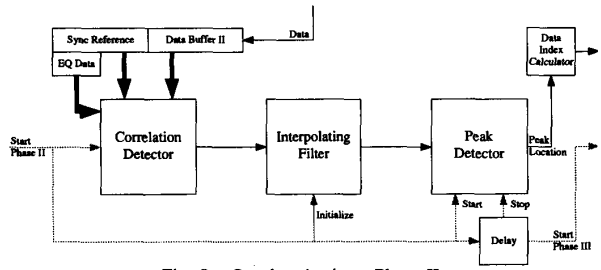

Fig. 9. Synchronization—Phase II.

As shown in Fig. 9, the received A/D samples are temporarily stored in Data Buffer II. At the start of Phase II, the last data value stored in Data Buffer I will also be the last data value stored in Data Buffer II. Initially, and each time a new data value is received, the correlation of the data in the buffer and the reference synchronization signal is determined. The reference signal is a copy of the transmitted synchronization signal.

The output of the correlation detector is input to an interpolating filter to provide a higher rate of samples. A peak detector monitors the output of the interpolating filter and records the location of the peak value. The peak detector resets and begins operation at the start of Phase II. Peak detection is halted a fixed time later. The duration of the peak detection process is chosen based on the performance of Phase I (see Section V-A). The peak location corresponds to the point of synchronization. The Data Index Calculator converts the output of the peak detector to an index pointer that identifies the location of the synchronized data block in the Main Data Buffer. The control signal that halts operation of the peak detector also initiates Phase III.

a) Correlation detector: To provide flexibility and adaptability at a modest computation load, the correlation detector was implemented in the frequency domain. To reduce the computational burden in transforming the data to the frequency domain, a special discrete Fourier transform (DFT) update routine was used.

The DFT update routine achieves a reduction in computational complexity by updating the spectral estimates based on previous estimates and by updating them only for the specific frequencies required. It is very effective for the correlation detector, which only requires the spectral information for the synchronization tones. The DFT update equation is

$$X_{n+1}(k) = [X_n(k) - x(n) + x(n+N)] \exp^{j(2k\pi/N)} \tag{2}$$

where N is the block size of the DFT/FFT, $x(n)$ is the nth data sample, and $X_n(k)$ is the spectral information of the kth sub-channel with the data window positioned between the nth and the $(n+N)$th data samples.

When Phase II is initiated, a previous spectral estimate does not exist. Therefore, the sync tone spectral information

Authorized licensed use limited to: Oxford University Libraries. Downloaded on March 31,2010 at 11:34:57 EDT from IEEE Xplore. Restrictions apply.

of the received data is calculated using a DFT or FFT.[3] Following this, the spectral estimates are updated using (2). A drawback of the DFT update routine is that round-off errors accumulate at each invocation of the routine. Therefore, the DFT/FFT should be used periodically to recalculate the spectral estimates.

Using the DFT update routine, the data in the Phase II data buffer is processed to extract the phase and magnitude of the sync tone sub-channels. To compensate for channel phase and magnitude distortions, the received sync tone phasors are multiplied by equalization phasors obtained as described in Section II-B.

The equalized phasors and the synchronization reference phasors are used to calculate the correlation detector output as

$$Y = \kappa \sum_{i=1}^{j} s_i \odot r_i \tag{3}$$

where s_i is the equalized phasor of the ith sync tone of the received signal; r_i is the phasor of the ith sync tone of the reference signal; j is the number of synchronization tones used; $\odot$ is the dot product; and κ is a constant.

b) Interpolation filter: The correlation detector provides snapshots, spaced at intervals equal to the sample period, of the continuous-time correlation between the received and reference synchronization signals. If the correlation function varies rapidly around its peak (this variation increases with the number of synchronization sub-carriers), the correlation detector output can be passed through a digital interpolation filter to obtain more frequent snapshots of the correlation and thus reduce the possibility of missing the correlation peak.

A 63-tap finite impulse response low pass filter was used to provide interpolated data values at four times the original data rate. This is sufficient to ensure that the peak is detected to within 95% of its actual value [21].

3) Phase III—Fine Synchronization: Since Phase II achieves synchronization to within $\pm\frac{1}{2}$ of a sample period, it is guaranteed that the data frame will be within the unweighted extensions (see Section IV-B) of the OFDM data frame. As shown in Fig. 10, an FFT is first performed on the received data frame. All sub-channels of the OFDM signal are then equalized to compensate for the known phase and magnitude distortions. Fine synchronization is performed on this final set of data. The algorithm derived in the Appendix calculates the time shift that maximizes the correlation with the reference synchronization signal. The required phase shift for each sub-channel is then calculated and applied prior to extracting the encoded data in the OFDM signal.

C. Selection of Synchronization Sub-channels

The selection of the sub-channels of the OFDM signal to be reserved for synchronization is critical to the performance of the synchronization algorithm. As with synchronization techniques for serial communications, the correlation functions for different synchronization signals have different side lobe patterns which affect synchronization performance.

[3]Depending on the number of sub-channels of interest, the DFT may be faster than the FFT.

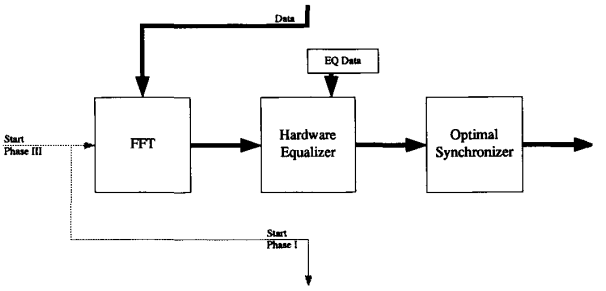

Fig. 10. Synchronization—Phase III.

Each sub-carrier of an OFDM signal has an integer number of periods in a frame duration. Since the synchronization signal is the sum of phase encoded sub-carriers, it will also have this property. We will refer to the period of the synchronization signal as the synchronization period. The exact number of synchronization periods in a frame duration depends on the specific sub-carriers used for synchronization.

In Phase II, the output of the correlation detector is monitored for a fixed period of time. If this period of time is greater than the synchronization period, two correlation peaks may result, causing synchronization errors. Therefore, the synchronization signal should have a period greater than the duration of the Phase II. Ideally, the J sub-carriers with a synchronization period greater than the minimum required and the minimum correlation sidelobe levels should be used. The number, J, of sub-channels needed for adequate performance was obtained from the experiments in Section V.

To facilitate the computation of the correlation function of the transmitted synchronization signal and the reference signal, two assumptions were made: (1) Distortion of the transmitted signal by the channel is negligible. (2) The pre-extension and post-extension of the transmitted signal (see Section IV-B) are each of duration at least $N/2$. A computer search based on this simplified model was run to determine the best J sub-channels. Initially, a brute force search to select 4 from the 256 available sub-channels was performed on a SUN SPARC Station 1. With 80% CPU utilization, the search took approximately seven days to complete. It was estimated that selecting 5 from the 256 available sub-channels would take 350 days to complete!

To reduce the search time, two simplifications were implemented:

1. Results from the initial searches with four synchronization sub-channels and different synchronization periods were examined. In all cases, it was found that each of the four sub-carriers selected had an integer (or close to an integer) number of periods in the minimum required periodic duration. Therefore, the search space was reduced to include only those sub-carriers that had an integer number of periods in the minimum required periodic duration.
2. The search was divided into a number of steps. At each step, the selected sub-channels from the previous step are kept, and an additional three sub-channels are selected that provide the smallest sidelobes.

Authorized licensed use limited to: Oxford University Libraries. Downloaded on March 31,2010 at 11:34:57 EDT from IEEE Xplore. Restrictions apply.

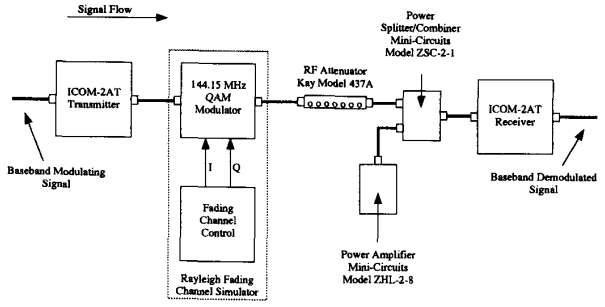

Fig. 11. FM fading channel.

IV. Experimental Set-Up

In this section, the laboratory experimental set-up used to measure the performance of the proposed synchronization scheme is described.

A. Analog FM Fading Channel

A block diagram depicting the implementation of the FM fading channel is given in Fig. 11. A baseband signal is used to modulate an ICOM-2AT FM transmitter. The RF signal is passed through a Rayleigh fading channel simulator [22]. The output from the fading simulator is passed through a step-wise variable attenuator and combined with the output of an RF noise source. The output of the power combiner is connected to the antenna input of the ICOM-2AT receiver.

1) Digital FM Channel: The digital FM channel shown in Fig. 4 is comprised of the analog FM fading channel shown in Fig. 11 and additional hardware and software, which allow for the input of data to the transmitter and output of data from the receiver to be in digital form.

The generation of the OFDM signal is shared between the host computer and special digital signal processing (DSP) hardware. The host is an IBM PC/AT compatible computer. Residing on the bus internal to the host is a DSP56001 Processor Board [23]. Connected to this board, and also residing on the host's internal bus, is a four-channel I/O board which provides Digital-to-Analog (D/A) and Analog-to-Digital (A/D) conversion [24].

a) OFDM signal generation: The sampling frequency of the system is set at 8 kHz, the Nyquist rate corresponding to a maximum signal frequency of 4 kHz. In the experiments, 256 frequency sub-channels between 1 kHz and 3 kHz are used to carry data and synchronization information. An IFFT of block size $N = 1024$ is used to construct the OFDM signal with these characteristics from the QAM encoded data. Within this block, data elements from 0 to 127 and from 384 to 511 are set to zero. The QAM encoded data is transferred to data elements 128 to 383. Data elements 512 to 1023 are defined to be the complex conjugates of elements 0 to 511. Data element 128 in the constructed data block corresponds to the 1-kHz frequency sub-channel of the OFDM signal. Data element 384 corresponds to the 3-kHz frequency sub-channel. Pre-emphasis of the encoded data by -10 dB per decade is provided in software to improve the performance of the system (see *Baseband Noise Power Spectrum* in Section II-B(4)).

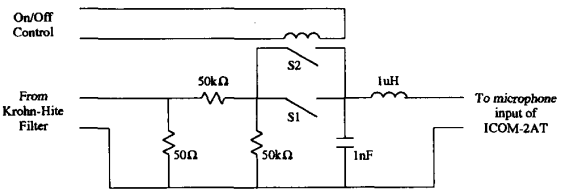

Fig. 12. Tx switch. S1—Manual Switch; S2—Voltage Controlled Switch

b) D/A loading factor: Prior to D/A conversion, the amplitude of the signal is modified to optimize the loading factor (LF) [25], defined as:

$$LF = \frac{\text{Peak amplitude}}{\text{RMS amplitude}}. \tag{4}$$

It was verified experimentally that a D/A loading factor of about 3.0 yielded good results. This was achieved by applying a software gain to the OFDM signal.

c) Gain and filtering: The reconstruction filter used in the experimental set-up was an 8th-order Butterworth low pass filter with a cutoff frequency of 4 kHz. As a precaution, an 8th-order high pass filter with a cutoff frequency of 100 Hz was used to remove any unexpected DC component from the signal.

The output signal of the D/A converter has a measured RMS level of 620 millivolts (RMS), whereas the desired level for the modulating signal is 6 millivolts (RMS). The necessary attenuation is provided by the Tx Gain unit, the filters, and the Tx switch.

d) Tx switch: The Tx switch, shown in Fig. 12, is used by the DSP hardware to turn the ICOM-2AT transmitter on or off. Within the ICOM-2AT transceiver, a load detector is attached to the microphone input. When a load is detected, the transmitter's Push To Talk (PTT) is enabled. When the load is removed, PTT is disabled. Based on the measured radio attack times of the ICOM-2AT's (see Section II-B), PTT is enabled 80 ms prior to the start of data transmission by the DSP.

e) Anti-aliasing filters: A 16th-order Butterworth low pass filter with a cutoff frequency of 4 kHz is used to remove all frequencies above 4 kHz to prevent aliasing.

f) Receiver gain: A receiver gain of 2.4 is used to achieve a signal level of 620 millivolts (RMS). For A/D sampling with a signal input range of ± 2.5 volts, this corresponds to a loading factor of 4.0.

g) Receiver software gain: In the transmitter, a software gain was applied to the signal to modify the loading factor. In the receiver, a reciprocal gain is applied to counteract this. Without this, processing of the data by the DSP will result in saturation and, therefore, distortion of the received data.

h) Channel equalization: Software equalization is performed to compensate for the amplitude and phase distortion caused by the digital FM channel hardware. Determination of the proper equalization is made through a training sequence procedure using the loop-back configuration described below. The results for ten transmissions of OFDM blocks generated from random data are processed and are shown in Fig. 13. The training procedure was performed periodically over the course

Authorized licensed use limited to: Oxford University Libraries. Downloaded on March 31,2010 at 11:34:57 EDT from IEEE Xplore. Restrictions apply.

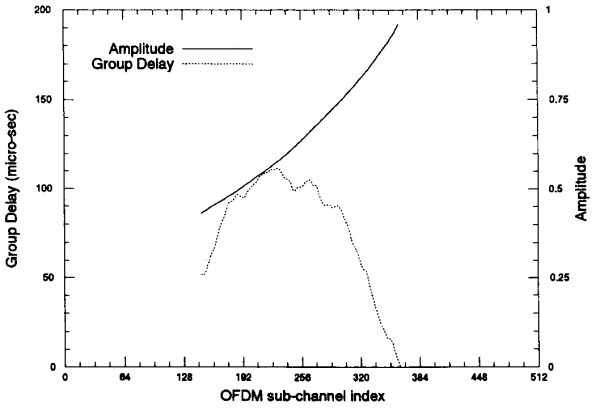

Fig. 13. Amplitude and group delay corrections for transmitted OFDM signal for a block size of 1024 with −10 -dB-per-decade pre-emphasis.

of the experiments; no significant change in the equalization transform was detected.

B. Raised Cosine Weighting Function

Transmission of the OFDM signal block is preceded by a 32-sample pre-extension and is followed by a 32-sample post-extension (see Transient Response in Section II-B(1)). To reduce transient effects further, the first 16 samples of the pre-extension and the last 16 samples of the post-extension are weighted by a raised cosine function. This provides a smooth transition in signal power from zero to full power during transmission of the pre-extension, and from full to zero power during transmission of the post-extension. The purpose of the post-extension is to reduce the effect of transients on an immediately following OFDM signal block.

C. Loop-Back and End-to-End Configurations

During the equalization training period and in several phases of experimentation, it is convenient to have perfect synchronization. This is achieved with a loop-back configuration, in which the host and its internal DSP processor board act as both transmitter and receiver. The clock that is used to trigger D/A conversion for the transmitter also triggers A/D conversion for the receiver.

For actual testing of the synchronization technique, the receiver must be unaware of transmitter timing. This is ensured by using an end-to-end configuration, in which data recovery is performed using a second host, operating independently of the transmitter.

D. Received Data Analyzer

In the experiments, five indicators are measured to judge synchronization performance: (1) bit error rate (BER); (2) probability of false alarm; (3) probability of miss detection; (4) probability of bad synchronization; and (5) probability of correct synchronization.

In the loop-back configuration, only the BER is meaningful, since ideal synchronization is available. In the end-to-end configuration, all five performance indicators are useful. To measure BER, the receiver's host is designed to generate a pseudo-random bit stream identical to that generated by the transmitter's host. Comparison of the generated bit stream and the received bit stream yields the BER. Determination of the other performance indicators is more involved and is detailed in [21].

TABLE I
EXPERIMENT LIST SUMMARY

IF S/N	Phase I	Phase II	Phase III	Integrated
10 dB	X Y Z	X Y _	X Y _	X Y _
15 dB	X __	X Y_	X Y _	X __
20 dB	X __	X __	X Y _	X Y_
25 dB	X Y Z	X __	X Y_	X Y _
X: f_d = 10 Hz		Y: f_d = 20 Hz		Z: f_d = 50 Hz

V. EXPERIMENTAL RESULTS

Experiments were conducted to measure the performance of each of the three phases of synchronization as well as that of the integrated system.

Table I summarizes the list of experiments: for Phase I with IF $S/N = 10$ dB, experiments were performed for Doppler rates of 10 Hz, 20 Hz, and 50 Hz; for Phase I with IF $S/N = 15$ dB, experiments were only performed for a Doppler rate of 10 Hz. In addition to these experiments, the test for probability of false alarm was performed, which is independent of the IF S/N and Doppler rate. The results from the experiments, together with the corresponding 95% confidence intervals [26], are presented below in graphical form.

A. Phase I Results

Phase I experimentation measures two performance indicators: (1) probability of false alarm and (2) accuracy of Phase I in locating the OFDM data frame.

Fig. 14 shows the performance of Phase I in the absence of a transmitted signal. From this, the probability of false alarm for a range of threshold levels can be predicted. During testing, 50 000 trials, each representing the transmission and reception of one OFDM data block, were performed for each indicated threshold level. During each trial, no RF carrier is present. The power of the demodulated baseband signal received from the FM receiver is estimated using 1024 samples of the received signal. Power estimation continues each time a new sample is received and concludes when a total of 1024 additional samples have been received. A false alarm is detected if any of the 1025 power estimations has a value less than the specified threshold.

For thresholds of 0.375 and lower, no false-alarm errors were detected. Later in this section it is shown that threshold levels of 0.15, 0.18, 0.21, and 0.25 are selected for IF S/N levels of 25 dB, 20 dB, 15 dB, and 10 dB, respectively. These thresholds are below the level for which false alarms were detected.

Figs. 15 and 16 show the performance of Phase I in the presence of a transmitted OFDM signal. The results

Authorized licensed use limited to: Oxford University Libraries. Downloaded on March 31,2010 at 11:34:57 EDT from IEEE Xplore. Restrictions apply.

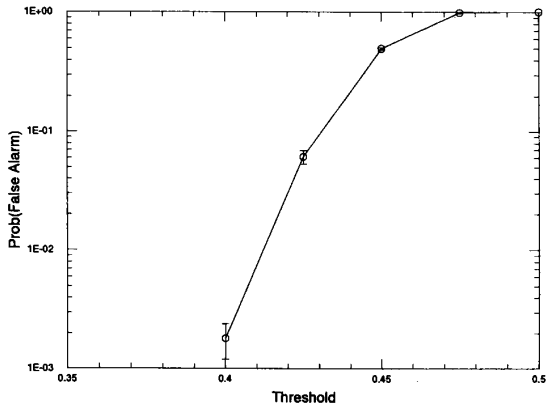

Fig. 14. Phase I performance in the absence of a transmitted signal.

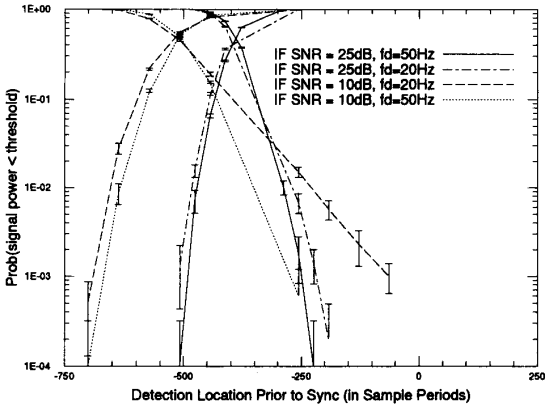

Fig. 16. Phase I performance in the presence of a transmitted signal. Doppler rates are $f_d = 20$ Hz and $f_d = 50$ Hz.

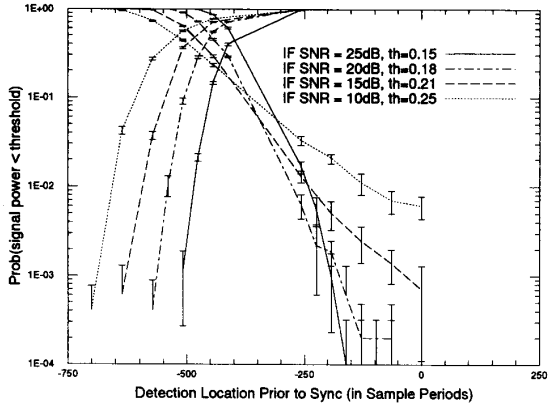

Fig. 15. Phase I performance in the presence of a transmitted signal. Doppler rate is $f_d = 10$ Hz.

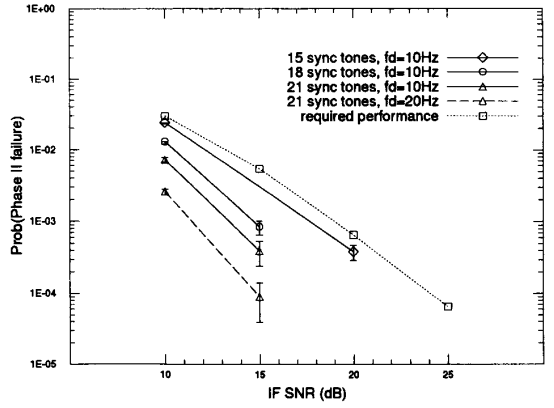

Fig. 17. Phase II performance.

are used to indicate the accuracy with which Phase I can determine the location of the OFDM data frame. Two sets of curves appear. The curves rising to the right give the probabilities that the estimated signal power drops below the threshold prior to that location. The horizontal axis indicates the location of detection prior to the start of the OFDM frame. The second set of curves (rising to the left) is generated by subtracting the first set from 1.0. They represent the probabilities that the estimated signal power does not drop below the threshold prior to that location. The threshold used for each IF S/N level is determined experimentally. The goal is to reduce the probability of detection occurring after the point of synchronization to satisfy the specified probability of miss sync. At the same time, the probability of detection at a point well before synchronization is to be reduced, since this will improve the conditions under which Phase II must operate.

The results of these experiments are used to determine the required duration of Phase II. For a given IF S/N, the location at which the curve rising to the right equals the required synchronization performance is determined. The distance from this location to the point of synchronization indicates the necessary duration of Phase II. This process is repeated for each IF S/N level. From the experimental results of Fig. 15, we conclude that a duration of 700 sample periods is sufficient to meet the required synchronization performance for all IF S/N levels of interest. Fig. 16 shows the effect of increasing the Doppler rate. A higher Doppler rate reduces the necessary duration of Phase II.

B. Phase II Results

Experiments were conducted to measure the probability that Phase II fails to achieve synchronization to within $\pm\frac{1}{2}$ of a sample period. Fig. 17 shows the probability of Phase II failure as a function of the IF S/N level for different numbers of synchronization tones and Doppler rates. Three curves appear for the Doppler setting of 10 Hz, corresponding to the use of 15, 18, and 21 synchronization tones. The sub-channels used for synchronization are listed in Table II and were obtained using the computer search discussed in Section III-C. The list of selected sub-channels in Table II is cumulative. For example, the sub-channels selected for 6 sync tones are $\{162, 246, 312, 170, 310, 358\}$. Comparing these curves with the reference curve indicating the required performance (also shown in the figure), it is apparent that

Authorized licensed use limited to: Oxford University Libraries. Downloaded on March 31,2010 at 11:34:57 EDT from IEEE Xplore. Restrictions apply.

TABLE II
SYNCHRONIZATION SUBCHANNEL SELECTION. OFDM BLOCK SIZE IS 1024; THEREFORE, AVAILABLE SUBCHANNELS ARE [0, 512]. OF THESE, ONLY [128, 384] ARE USED

Number of Sync Tones	Selected Sub-channels (cumulative)
3	162 246 312
6	170 310 358
9	176 214 256
12	206 230 370
15	132 190 224
18	140 234 372
21	184 276 344

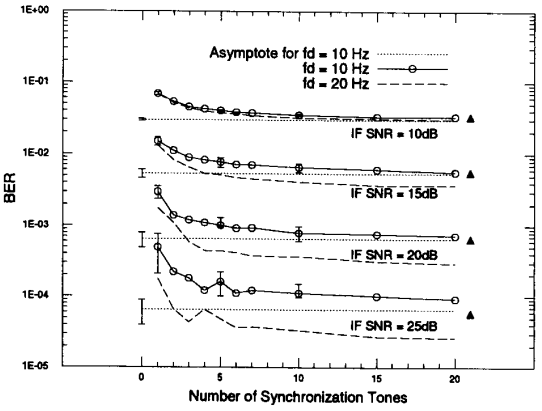

Fig. 18. Phase III performance—absolute results.

the specified requirements can be met using 15 sync tones. Also appearing in Fig. 17 is a performance plot for 21 sync tones and a Doppler rate of 20 Hz. The effect of increasing the Doppler rate from 10 Hz to 20 Hz results in a 2-dB improvement.

C. Phase III Results

Phase III experimentation measures the ability of the fine-tune algorithm to acquire synchronization accurately. This ability is measured indirectly by comparing the BER resulting from fine-tune synchronization with the BER that could be obtained assuming ideal synchronization.

Figs. 18 and 19 present the experimental results. In Fig. 18, the dotted curves represent the best achievable BER for a Doppler rate of 10 Hz, obtained when ideal synchronization is achieved. Fig. 19 displays the same data as Fig. 18, but as a ratio of actual BER compared to the BER for ideal synchronization. Except for the case of IF $S/N = 25$ dB, the relative results are quite similar. Also shown is the BER performance requirement curve. In general, fine-tune synchronization improves as the number of synchronization tones is increased. The rate of improvement is greatest when the number of tones is small. When six or more synchronization tones are used, the performance of the fine-tune algorithm exceeds the requirements.

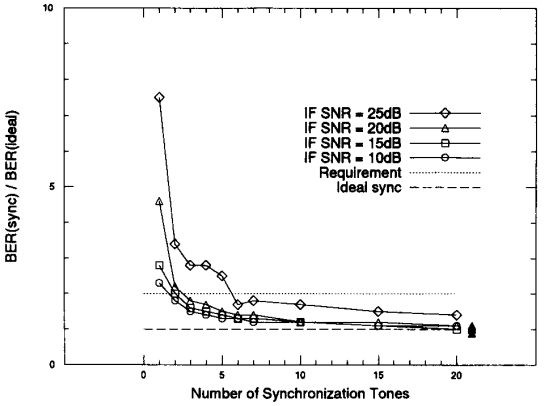

Fig. 19. Phase III performance—relative to ideal. $f_d = 10$ Hz.

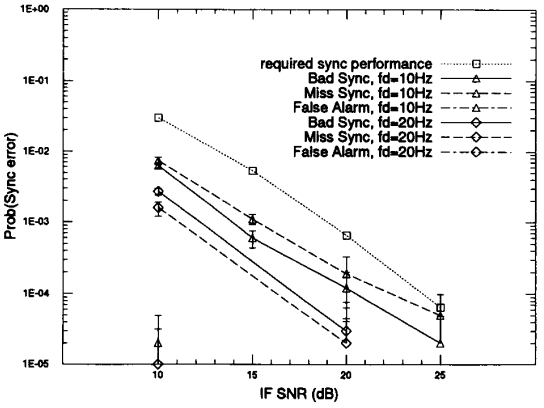

Fig. 20. Integrated system synchronization performance.

The effect of increasing the Doppler rate is shown in Fig. 18 by the dashed lines. Negligible improvement results for IF $S/N = 10$ dB. The degree of improvement increases with increasing IF S/N. For IF $S/N = 25$ dB, increasing the Doppler rate from 10 Hz to 20 Hz reduces the BER by a factor of three when seven or more synchronization tones are used.

Integrated testing, presented in the following section, uses 21 synchronization tones for Phase II and uses all of them again for Phase III. The performance of Phase III using these synchronization tones is identified by the solid triangles in Figs. 18 and 19.

D. Integrated Results

The results of the integrated system tests are given in Figs. 20, 21, and 22. For each test case, 100 000 trials were conducted.

Fig. 20 shows the performance of the synchronization algorithm with respect to the probability of bad synchronization, the probability of missed synchronization, and the probability of false alarm. For IF S/N levels of 15 dB or more, no false alarms were detected. For 25-dB IF S/N and 20-Hz Doppler rate, no synchronization errors at all were detected. The results show that the achieved synchronization performance is better

Authorized licensed use limited to: Oxford University Libraries. Downloaded on March 31,2010 at 11:34:57 EDT from IEEE Xplore. Restrictions apply.

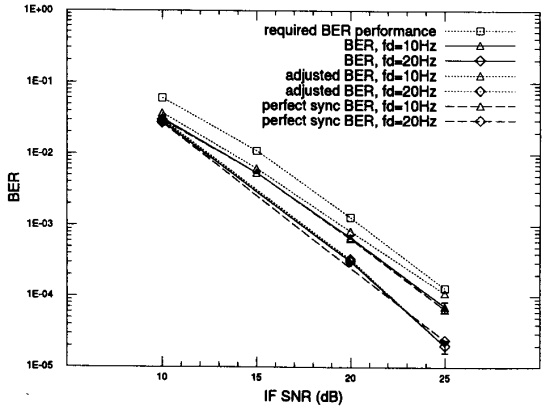

Fig. 21. Integrated system BER performance.

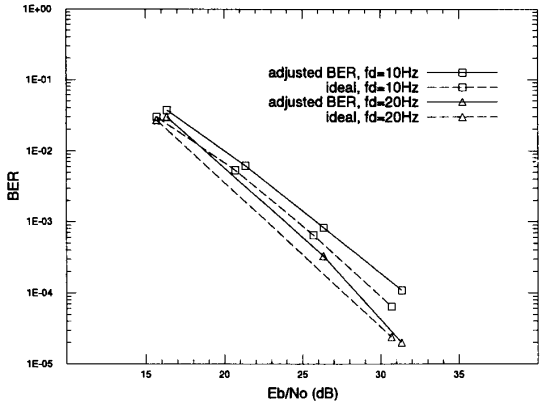

Fig. 22. Performance loss due to synchronization.

than the specified requirements. For 10-dB IF S/N and 10-Hz Doppler, this margin is approximately 4 dB. An increase in the Doppler rate to 20 Hz improves performance by an additional 4 dB.

Fig. 21 shows the resulting BER performance. Two sets of curves appear. One set indicates BER when only correctly synchronized OFDM blocks are considered. The second set of curves has been adjusted to indicate BER performance when incorrectly synchronized OFDM blocks are included. In adjusting the BER, it is assumed that incorrectly synchronized blocks have a block BER of 1/2.

The specified BER requirements are met by both the adjusted and unadjusted BER measurements. For a 10-Hz Doppler rate, the BER performance is more than 1.5 dB better than the specified requirements. An additional 1.5-dB performance gain is obtained when the Doppler rate is increased to 20 Hz.

The specification of synchronization performance in Section III-A is somewhat arbitrary, so that comparison of actual performance with the specified requirements is a bit artificial. To provide another indication of the synchronization performance, the BER was plotted as a function of E_b/N_o, where E_b is the average received energy per bit, and N_o is the noise power spectral density [27].

Fig. 22 shows the adjusted BER results. The ideal performance curves are also shown to provide a reference from which the performance loss due to synchronization is measured. The ideal curves are determined based on the assumptions of ideal synchronization and no overhead required for synchronization information or for periodic extensions.

The curves in Fig. 22 show that for both the 10-Hz and 20-Hz Doppler rate, the use of the proposed synchronization scheme results in a BER performance that is approximately 1.5 dB worse than the BER performance with ideal synchronization. Increasing the Doppler rate from 10 Hz to 20 Hz results in a 2-dB improvement in BER performance.

VI. Conclusions

A technique for acquiring individual frame synchronization in an OFDM/FM system operating in a pure ALOHA environment has been designed, implemented, and tested experimentally. The required bandwidth overhead is less than 10%. The results also indicate that the BER performance achievable with this technique is within 1.5 dB of the performance assuming ideal synchronization.

Appendix
Fine-Tune Algorithm

In this appendix, we discuss the calculation of the time shift, τ, used in Phase III to maximize the correlation, $\mathcal{R}_{rs}(\tau)$, of the received signal $s(t)$ and the reference synchronization signal $r(t)$. Since Phase II achieves synchronization to within half a sample period, we are interested only in evaluating the correlation over a small range of the scanning parameter τ. In this case, a relatively simple expression for $\mathcal{R}_{rs}(\tau)$ can be obtained [21], namely

$$\mathcal{R}_{rs}(\tau) = \frac{T}{2}\sum_{i=1}^{N_s}\cos(\omega_i\tau + \theta_i), \tag{5}$$

where ω_i is the angular frequency of the ith sync tone, and θ_i represents the phase difference between the ith received and reference sync tones. The derivative of $\mathcal{R}_{rs}(\tau)$ is given by

$$\frac{d\mathcal{R}_{rs}(\tau)}{d\tau} = -\frac{T}{2}\sum_{i=1}^{N_s}\omega_i\sin(\omega_i\tau + \theta_i). \tag{6}$$

For most acceptable IF S/N values, we would expect $(\omega_i\tau + \theta_i)$ to be small. In such cases, from (6) we can write

$$\frac{d\mathcal{R}_{rs}(\tau)}{d\tau} \approx -\frac{T}{2}\sum_{i=1}^{N_s}\omega_i(\omega_i\tau + \theta_i). \tag{7}$$

The time shift τ^* for which the derivative is zero then satisfies

$$0 \approx \sum_{i=1}^{N_s}\omega_i(\omega_i\tau^* + \theta_i), \tag{8}$$

Authorized licensed use limited to: Oxford University Libraries. Downloaded on March 31,2010 at 11:34:57 EDT from IEEE Xplore. Restrictions apply.

so that

$$\tau^* \approx -\frac{\sum_{i=1}^{N_s} \omega_i \theta_i}{\sum_{i=1}^{N_s} \omega_i^2}. \quad (9)$$

REFERENCES

[1] W. C. Y. Lee, *Mobile Cellular Telecommunications Systems.* New York: McGraw-Hill, 1989.

[2] D. C. Cox, "Universal digital portable radio communications," *Proc. IEEE,* vol. 75, pp. 436–477, Apr. 1987.

[3] D. C. Cox, "A radio system proposal for widespread low-power tetherless communications," *IEEE Trans. Commun.,* vol. 39, pp. 324–335, Feb. 1991.

[4] R. H. Clarke, "A statistical theory of mobile-radio reception," *Bell Syst. Tech. J.,* vol. 47, pp. 957–1000, Jul.–Aug. 1968.

[5] W. C. Jakes, ed., *Microwave Mobile Communications.* New York: Wiley, 1974.

[6] F. Hansen and F. Meno, "Mobile fading—Rayleigh and lognormal superimposed," *IEEE Trans. Veh. Technol.,* vol. VT-26, pp. 332–335, Nov. 1977.

[7] L. J. Cimini, "Analysis and simulation of a digital mobile channel using orthogonal frequency division multiplexing," *IEEE Trans. Commun.,* vol. COM-33, pp. 665–675, July 1985.

[8] E. Casas and C. Leung, "OFDM for data communication over mobile radio FM channels, part I: analysis and experimental results," *IEEE Trans. Commun.,* vol. 39, pp. 783–793, May 1991.

[9] B. R. Salzberg, "Performance of an efficient parallel data transmission system," *IEEE Trans. Commun. Tech.,* vol. COM-15, pp. 805–811, Dec. 1967.

[10] S. B. Weinstein and P. M. Ebert, "Data transmission by frequency-division multiplexing using the discrete Fourier transform," *IEEE Trans. Commun. Technol.,* vol. COM-19, pp. 628–634, Oct. 1971.

[11] J. A. C. Bingham, "Multicarrier modulation for data transmission: An idea whose time has come," *IEEE Commun. Mag.,* pp. 5–14, May 1990.

[12] *IC-2A/AT/E 144 MHz FM Transceiver Maintenance Manual,* ICOM Inc., unpublished.

[13] *Minimum standards for land mobile communication FM or PM transmitters, 25-470 MHz,* EIA Standard RS-152-B, Feb. 1970.

[14] *Minimum standards for land mobile communication FM or PM receivers, 25-947 MHz,* EIA Standard RS-204-C, Jan. 1982.

[15] *Minimum standards for portable/personal radio transmitters, receivers, and transmitter/receiver combination land mobile communications FM or PM equipment, 25-1000 MHz,* EIA Standard RS-316-B, May 1979.

[16] R. G. Gallager, *Information Theory and Reliable Communication.* New York: Wiley, 1968.

[17] B. Hirosaki, "A 19.2 kbps voiceband data modem based on orthogonally multiplexed QAM techniques," in *Proc. IEEE Int. Conf. Commun.,* 1985, Chicago, IL, June 23–26, 1985, pp. 21.1.1–21.1.5 or 661–665.

[18] W. E. Keasler, "Reliable data communication over the voice bandwidth telephone channel using orthogonal frequency division multiplexing," Ph.D. dissertation, Univ. Illinois at Urbana-Champaign, 1982.

[19] P. Baran, "Packetized ensemble modem," U.S. Patent 4 438 511, Mar. 1984.

[20] P. H. Moose, "Differential modulation and demodulation of multi-frequency digital communications signals," in *MILCOM 90,* pp. 273–277 or 12.4.1–12.4.5, Oct. 1990.

[21] W. D. Warner, "OFDM/FM frame synchronization for mobile radio data communication," M.A.Sc. thesis, Univ. of British Columbia, 1991.

[22] E. F. Casas and C. Leung, "A simple digital fading simulator for mobile radio," *IEEE Trans. Veh. Technol.,* vol. 39, pp. 205–212, Aug. 1990.

[23] *DSP56001 Processor Board User's Manual,* Spectrum Signal Processing Inc., version 2 ed., Oct. 1988.

[24] *4 Channel Analog I/O Board User's Manual,* Spectrum Signal Processing Inc., version 2.1 ed., Nov. 1988.

[25] N. S. Jayant and P. Noll, *Digital Coding of Waveforms: Principles and Applications to Speech and Video.* Englewood Cliffs, NJ: Prentice-Hall, 1984.

[26] P. G. Moore and E. A. C. Shirley, *Standard Statistical Calculations.* New York: Wiley, 1972.

[27] R. E. Ziemer and W. H. Tranter, *Principles of Communications: Systems, Modulation and Noise.* Boston, MA: Houghton Mifflin, 1985.

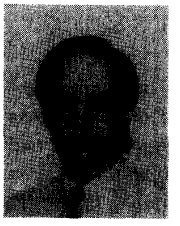

William D. Warner received the B.A.Sc. degree in systems design engineering from the University of Waterloo, Ontario, Canada in 1986, and the M.A.Sc. degree in electrical engineering from the University of British Columbia, Vancouver, Canada, in 1991.

From 1986 to 1988, he worked for Diffracto, Ltd., a machine vision research and development company located in Windsor, Ontario. Since 1991, he has been with MPR Teltech Ltd. in Burnaby, BC, Canada, where he is a member of the technical staff in the Wireless Division. His current activities include spread spectrum communications and DSP modem design.

Mr. Warner is a member of the Association of Professional Engineers of Ontario.

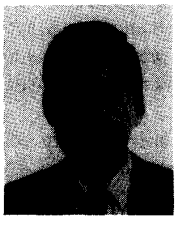

Cyril Leung (S'74–M'76) received the B.Sc. (honours) degree from Imperial College, University of London, UK, in 1973, and the M.S. and Ph.D. degrees in electrical engineering from Stanford University in 1974 and 1976, respectively.

From 1976 to 1979 he was an Assistant Professor in the Department of Electrical Engineering and Computer Science, Massachusetts Institute of Technology. He was on leave during 1978 at Bell Laboratories, Holmdel, NJ, working on data networks. During 1979 to 1980 he was with the Department of Systems Engineering and Computing Science, Carleton University, Ottawa, Canada. Since 1980, he has been with the Department of Electrical Engineering, University of British Columbia, Vancouver, BC, Canada, where he is a Professor. In 1987, he was on sabbatical leave in the Department of Electrical Engineering, Ecole Polytechnique de Montreal, Montreal, PQ, Canada. His current research interests are in mobile radio data communications, coding, and data security.

Dr. Leung is a member of the Association of Professional Engineers of Ontario.

Authorized licensed use limited to: Oxford University Libraries. Downloaded on March 31,2010 at 11:34:57 EDT from IEEE Xplore. Restrictions apply.